The Plant Cell, Vol. 16, 3098–3109, November 2004, www.plantcell.org

Colocalization of L-Phenylalanine Ammonia-Lyase and Cinnamate 4-Hydroxylase for Metabolic Channeling in Phenylpropanoid Biosynthesis

Lahoucine Achnine, Elison B. Blancaflor, Susanne Rasmussen,[1] and Richard A. Dixon[2]

Plant Biology Division, Samuel Roberts Noble Foundation, Ardmore, Oklahoma 73401

Metabolic channeling has been proposed to occur at the entry point into plant phenylpropanoid biosynthesis. To determine whether isoforms of L-Phe ammonia-lyase (PAL), the first enzyme in the pathway, can associate with the next enzyme, the endomembrane-bound cinnamate 4-hydroxylase (C4H), to facilitate channeling, we generated transgenic tobacco (*Nicotiana tabacum*) plants independently expressing epitope-tagged versions of two PAL isoforms (PAL1 and PAL2) and C4H. Subcellular fractionation and protein gel blot analysis using epitope- and PAL isoform-specific antibodies indicated both microsomal and cytosolic locations of PAL1 but only cytosolic localization of PAL2. However, both PAL isoforms were microsomally localized in plants overexpressing C4H. These results, which suggest that C4H itself may organize the complex for membrane association of PAL, were confirmed using PAL-green fluorescent protein (GFP) fusions with localization by confocal microscopy. Coexpression of unlabeled PAL1 with PAL2-GFP resulted in a shift of fluorescence localization from endomembranes to cytosol in C4H overexpressing plants, whereas coexpression of unlabeled PAL2 with PAL1-GFP did not affect PAL1-GFP localization, indicating that PAL1 has a higher affinity for its membrane localization site than does PAL2. Dual-labeling immunofluorescence and fluorescence energy resonance transfer (FRET) studies confirmed colocalization of PAL and C4H. However, FRET analysis with acceptor photobleaching suggested that the colocalization was not tight.

INTRODUCTION

Phenylpropanoid plant natural products are important for both plant and animal health (Dixon et al., 1999, 2002; Dixon and Sumner, 2003). They are derived from *trans*-cinnamic acid formed by deamination of L-Phe by L-Phe ammonia-lyase (PAL; EC 4.3.1.5). PAL is a tetrameric enzyme whose subunits are encoded by multigene families in most species studied (Cramer et al., 1989; Nagai et al., 1994; Wanner et al., 1995; Fukasawa-Akada et al., 1996). In tobacco (*Nicotiana tabacum*), *PAL* genes have a simple organization consisting of two families, each with two very closely related genes (Nagai et al., 1994; Pellegrini et al., 1994). Tobacco PAL1 and PAL2, representatives of the two PAL families, share 82% amino acid identity (Figure 1A).

Routes to the major classes of phenylpropanoid compounds involve the core phenylpropanoid pathway from Phe to an activated (hydroxy) cinnamic acid derivative via the actions of PAL, cinnamate 4-hydroxylase (C4H; EC 1.14.13.11, a cytochrome P450) and 4-coumarate:CoA ligase, and specific branch pathways for the formation of monolignols/lignin, sinapate esters, condensed tannins, anthocyanins, coumarins, benzoic acids, flavonoids/isoflavonoids, and stilbenes (Dixon et al., 2002).

Phenylpropanoid biosynthesis comprises several groups of reactions through which metabolic channeling may occur (Winkel, 2004). This phenomenon involves the physical organization of successive pathway enzymes into complexes through which metabolic intermediates are channeled without diffusion into the bulk of the cytosol (Srere, 1987). Such complexes are loose, however, and many of the component enzymes may be operationally soluble. Channeling allows for efficient control of metabolic flux and protects unstable intermediates from nonproductive breakdown or access to enzymes from potentially competing pathways. It may involve direct physical interactions between the component enzymes, as demonstrated for enzymes of flavonoid biosynthesis in *Arabidopsis thaliana* (Winkel-Shirley, 1999), and/or may be associated with colocalization of enzymes on membranes or other surfaces (Hrazdina and Wagner, 1985a; Liu and Dixon, 2001).

Channeled intermediates are often less efficient precursors of downstream products than are their upstream substrates, and by this and other criteria, channeling of *trans*-cinnamic acid between PAL and C4H has been demonstrated (Czichi and Kindl, 1975; Hrazdina and Wagner, 1985a; Hrazdina and Jensen, 1992; Rasmussen and Dixon, 1999). The membrane-associated C4H cytochrome P450 might act to anchor a complex consisting of PAL, and possibly other phenylpropanoid pathway enzymes, to the endoplasmic reticulum (ER). Preliminary cell fractionation

[1] Current address: AgResearch, Tennent Drive, Private Bag 11008, Palmerston North, New Zealand.

[2] To whom correspondence should be addressed. E-mail radixon@noble.org; fax 580-224-6692.

The author responsible for distribution of materials integral to the findings presented in this article in accordance with the policy described in the Instructions for Authors (www.plantcell.org) is: Richard A. Dixon (radixon@noble.org).

Article, publication date, and citation information can be found at www.plantcell.org/cgi/doi/10.1105/tpc.104.024406.

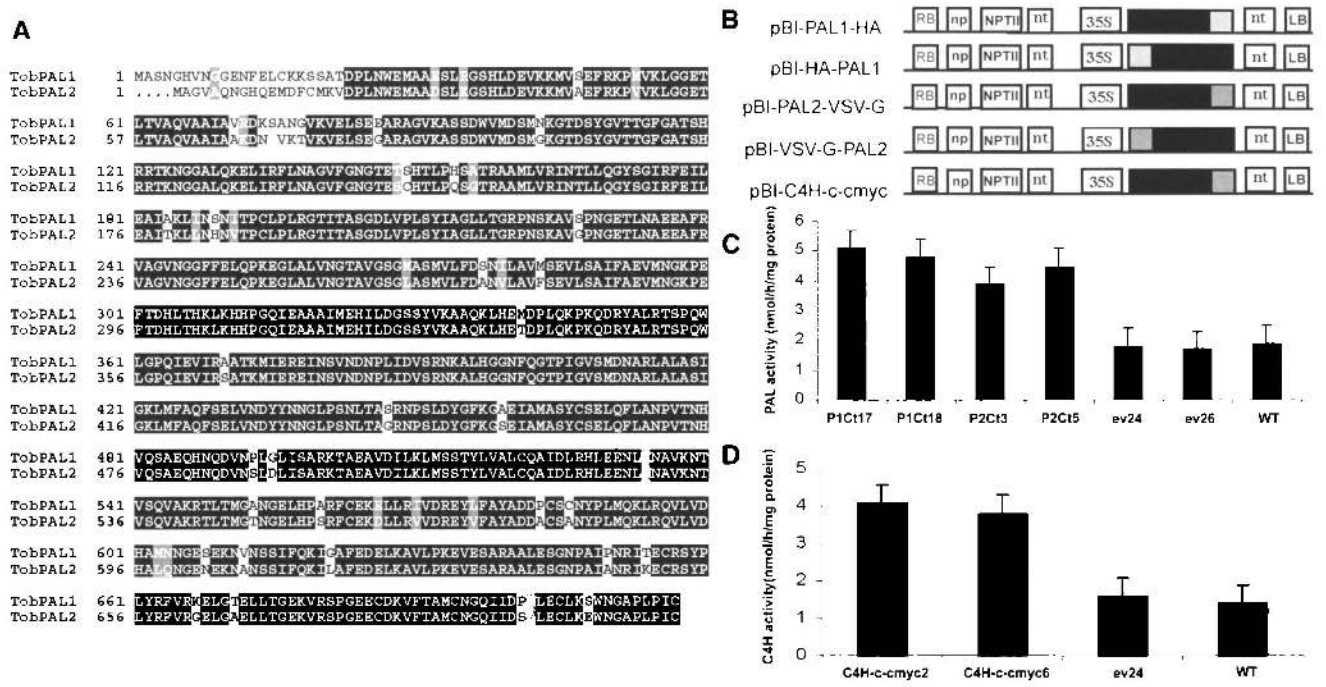

Figure 1. Expression of Epitope-Tagged PAL and C4H Constructs in Transgenic Tobacco.

(A) Alignment of tobacco PAL1 and PAL2 proteins using the ClustalW sequence alignment program of the Lasergene software package (DNASTAR, Madison, WI) and Boxshade (http://www.ch.embnet.org/software/BOX_form.html).

(B) Constructs used for plant transformation. PAL and C4H open reading frames (black bars) were fused to epitope peptides (gray bars) at the N or C termini. Epitopes were HA epitope (YPYDVPDYA, from human influenza hemagglutinin protein), VSV-G epitope (YTDIEMNRLGK from vesicular stomatitis virus glycoprotein), and c-myc epitope (EQKLISEEDL from human c-myc protein). Constructs were in binary vector pBI121 under control of the 35S promoter of *Cauliflower mosaic virus* (35S) with nopaline synthase terminator (nt).

(C) and **(D)** Extractable activities of PAL **(C)** and C4H **(D)** in transgenic tobacco lines expressing epitope-tagged PAL1, PAL2, or C4H constructs. ev, empty vector transformed; WT, wild-type plants (nontransformed). Data are means and standard deviations from three independent assays for each line.

studies suggest that PAL1, but not PAL2, is localized to the ER in the wild-type tobacco cells (Rasmussen and Dixon, 1999). However, it is still not clear whether direct physical interactions exist between PAL and C4H. To address this question, we generated transgenic tobacco plants expressing epitope-tagged PAL and C4H gene fusion constructs. Using subcellular fractionation, protein gel blot analysis, in vivo localization using green fluorescent protein (GFP), immunofluorescence, and fluorescence resonance energy transfer (FRET) techniques, we have demonstrated colocalization of PAL and C4H on ER membranes in tobacco. Overexpression of C4H results in reorganization of PAL2 localization from cytosol to ER.

RESULTS

Generation of Transgenic Plants with Epitope-Tagged PAL or C4H

Five constructs (pBI-PAL1-HA, pBI-HA-PAL1, pBI-PAL2-VSV-G, pBI-VSV-G-PAL2, and pBI-C4H-c-myc) were made for transformation of tobacco with N-terminal or C-terminal epitope-tagged PAL1 or PAL2 or with C-terminal epitope-tagged C4H, all open reading frames being under control of the constitutive 35S promoter (Figure 1B). Ten independent C4H-c-myc transgenic lines, 12 independent HA epitope-tagged PAL1 lines, 10 VSV-G epitope-tagged PAL2 lines, and five empty-vector (ev) control lines were identified based on PCR analysis using primers specific for the 35S promoter. DNA gel blot analysis revealed that lines P1Ct17 and P1Ct18 (harboring PAL1 C-terminal epitope fusions) and P2Ct3 and P2Ct5 (harboring PAL2 C-terminal epitope fusions) contained one or two transgene inserts, whereas the C4H-c-myc2 and C4H-c-myc6 lines contained multiple *C4H* transgene copies (data not shown). These six lines were used for further analysis of PAL/C4H colocalization.

Extractable PAL activities in leaves of epitope-tagged PAL1 and PAL2 transgenic plants were ~2.5-fold higher than in corresponding empty-vector or the wild-type lines (Figure 1C). Similarly, C4H-c-myc–expressing plants exhibited an ~2.5-fold increase in extractable C4H activity (Figure 1D).

Subcellular Localization of PAL and C4H as Determined by Protein Gel Blot Analysis

Protein extracts from leaves of transgenic plants harboring epitope-tagged PAL and C4H constructs were fractionated by

differential centrifugation to obtain total, microsomal, and soluble fractions. Protein gel blot analysis using PAL1 peptide-specific antibodies (Figure 2A) and anti-HA epitope antibodies (Figure 2B) showed that PAL1 was present in both microsomal and soluble fractions, whereas PAL2 was present only in the total and soluble fractions (Figures 2C and 2D). As would be predicted for a cytochrome P450 (Chapple, 1998), C4H-c-myc protein detected by anti-(c-myc) serum was exclusively found in the microsomal fraction (Figure 2E). Anti-PAL1 and anti-PAL2 antibodies, but not anti-HA and anti-VSV-G, detected endogenous PAL1 and PAL2 proteins in the empty-vector controls ev24 and ev26 (Figures 2A to 2D).

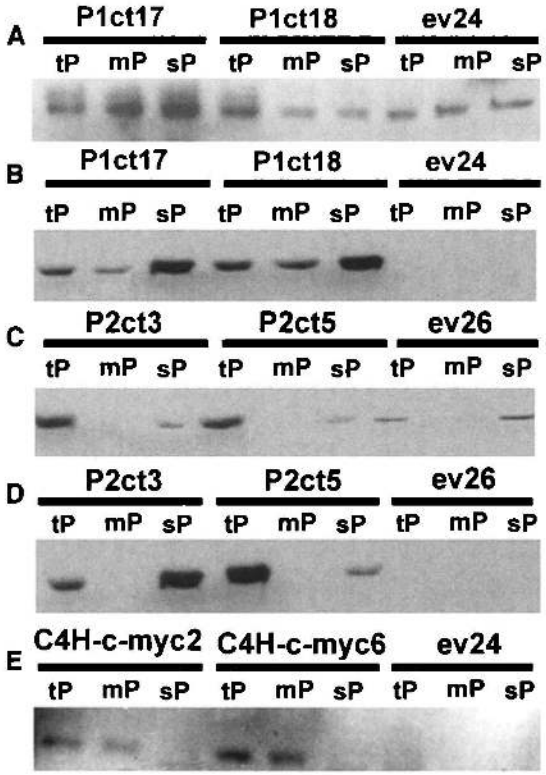

Figure 2. Subcellular Distribution of PAL and C4H Proteins Determined by Protein Gel Blot Analysis.

Protein levels were measured in the total (tP), microsomal (mP; 130,000*g* pellet), and soluble (sP; 130,000*g* supernatant) fractions from transgenic and empty-vector control lines (15 μg protein per lane).

(A) and **(B)** Tobacco PAL1 protein detected using anti-(tobacco PAL1) serum **(A)** and HA epitope-tagged tobacco PAL1 protein detected using anti-HA epitope antibody **(B)**. P1ct17 and P1ct18 are HA-PAL1 expressing lines.

(C) and **(D)** Tobacco PAL2 protein detected using anti-(tobacco PAL2) serum **(C)** and VSV-G epitope-tagged tobacco PAL2 protein identified using anti-VSV-G epitope antibody **(D)**. P2ct3 and P2ct5 are VSV-G-PAL2–expressing lines.

(E) c-myc epitope-tagged tobacco C4H protein identified using anti-c-myc epitope antibody. C4H-c-myc2 and C4H-c-myc6 are C4H-c-myc–expressing lines.

Localization of PAL1, PAL2, and C4H in Vivo Using GFP Fusions

The subcellular localization of PAL1 and PAL2 was further investigated using enhanced GFP (eGFP) as reporter in transient expression assays with PAL-eGFP and C4H-eGFP fusions in tobacco leaf epidermal cells. Figure 3 shows confocal images of fluorescence resulting from bombardment of GFP fusion constructs into leaves of the wild-type plants. Constructs expressing eGFP and eGFP-HDEL (harboring a C-terminal ER retention signal) served as controls (Haseloff et al., 1997). Fluorescence from unmodified eGFP was observed throughout the cytoplasm and nucleus, and cell organelles appeared as dark zones against this background (Figure 3A). Expression of eGFP-HDEL resulted in display of the ER (Figure 3B), and the same reticulate pattern of eGFP signal distribution was observed following transient expression of the C4H-MA-eGFP protein in which the C4H N-terminal membrane anchor (MA) alone was fused to eGFP (Figure 3C). Transient expression of the PAL1-eGFP fusion protein resulted in a reticulate distribution of fluorescence in 10 out of 10 cells examined (Figure 3D), although a portion of the protein is clearly cytoplasmically localized, consistent with the subcellular fractionation studies. By contrast, the localization of PAL2-eGFP appeared wholly cytosolic in seven out of seven cells examined (Figure 3E). These data independently confirm the differential subcellular localization of PAL1 and PAL2 revealed by biochemical fractionation and protein gel blot analyses.

To address whether C4H is itself a binding partner, or an essential component, for localizing operationally soluble PAL to the ER, PAL1-eGFP and PAL2-eGFP constructs were bombarded into young leaves from plants overexpressing C4H-c-myc. Localization of both PAL1-eGFP and PAL2-eGFP was now strongly reticulate in 100% of the cells examined (Figures 4A and 4B), similar to the localization of eGFP-HDEL (Figure 3B) and C4H-MA-eGFP (Figure 3C). This altered relative distribution of the two PAL forms in C4H-overexpressing plants was confirmed for endogenous PAL1 and PAL2 by protein gel blot analysis with detection using PAL isoform-specific antisera (Figures 5B and 5C); unlike the situation in extracts from empty-vector control plants (Figures 2 and 5C), PAL2 was now detected in the microsomal fraction (Figure 5C). Note that a significant proportion of both PAL proteins was, however, still found in the soluble fraction.

The above results suggest that the affinity of PAL1 for its ER target site is greater than the affinity of PAL2 for this site. To test this hypothesis, leaves of C4H-overexpressing plants were cobombarded with PAL1-eGFP and unmodified PAL2 or with PAL2-eGFP and unmodified PAL1. All signal from PAL1-eGFP was in a reticulate pattern when the fusion protein was coexpressed with unmodified PAL2 in 14 out of 14 cells examined (Figure 4C), demonstrating that PAL2 could not compete with PAL1 for ER association. However, when PAL1 was cobombarded with PAL2-eGFP under the same conditions, the distribution of GFP fluorescence initially resembled the ER network in 12 out of 13 cells examined. However, by 15 h after bombardment, the fluorescence was cytosolic in all the cells (Figure 4E). The cell shown in Figure 4D was observed 11 h after bombardment, whereas Figure 4E shows a cell after 15 h. In a second set of

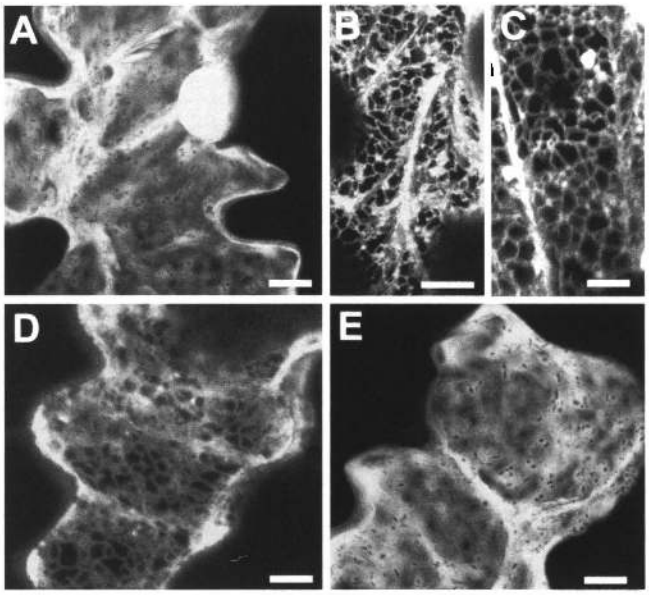

Figure 3. In Vivo Localization of PAL- and C4H-eGFP Fusion Proteins in Leaf Epidermal Cells of the Wild-Type Tobacco Plants.

Transient expression of free eGFP **(A)**, eGFP-HDEL **(B)**, C4H-MA-eGFP **(C)**, PAL1-eGFP **(D)**, and PAL2-eGFP **(E)** was achieved by bombardment of the corresponding expression constructs. Note the reticulate pattern of localization for eGFP-HDEL, PAL1-eGFP, and C4H-MA-eGFP. Bars = 10 μm in **(A)** and **(C)** to **(E)** and 20 μm in **(B)**.

experiments with C4H-overexpressing plants, PAL2-eGFP was cytosolically localized at 12 h after cobombardment with PAL1 in 20 out of 20 cells examined. Thus, loss of ER-localized fluorescence is repeatedly observed in cells coexpressing PAL1 and PAL2-eGFP, whereas ER-localized fluorescence from PAL1-eGFP remains stable after cobombardment with unlabeled PAL2. Thus, PAL1 exhibits a greater affinity than PAL2 for the ER binding site(s).

Analysis of PAL/C4H Colocalization

The above data, although pointing to C4H or some other protein associated with C4H as the binding partner that localizes operationally soluble PAL isoforms to the ER, do not give any indication of how closely PAL and C4H might be colocalized. To address this question, double-immunolabeling studies were performed on tobacco protoplasts overexpressing C4H-c-myc. Protoplasts were used to optimize fixation and imaging of the delicate endomembrane structures to which PAL isoforms associate.

Double labeling of the protoplasts with antibodies against PAL1, PAL2, and c-myc, with secondary antibodies conjugated to Alexa Fluor-488 and Texas Red, confirmed the GFP data in Figure 4. The fluorescence localization pattern of both PAL isoforms (Figures 6A and 6D) and C4H (Figures 6B and 6E) resembled the reticulate ER network previously observed in protein localization studies in tobacco protoplasts (Heinlein et al., 1998; Frigerio et al., 2001). To quantify the degree of colocalization between PAL and C4H, merged images obtained from single optical sections of double-labeled samples for PAL1 and C4H (Figure 6C) and PAL2 and C4H (Figure 6F) were analyzed using LaserSharp colocalization software. Scattergrams were generated from the merged images that display the intensity and distribution of red and green pixels, and a colocalization coefficient (Manders et al., 1993) was calculated for each colored fluorophore (Figures 6G and 6H). For a particular color (e.g., red), the colocalization coefficient represents the ratio of red pixel intensities showing a green component divided by the sum of all red intensities. A value of zero means no colocalization, whereas a value of one indicates complete colocalization (Smallcombe, 2001). For PAL1 and C4H, colocalization coefficients of 0.99 and 0.97 were obtained for red (C4H) and green (PAL1) pixels, respectively (Figure 6G). Similarly, PAL2 and C4H-labeled samples showed coefficients of 0.99 for red and 0.94 for green pixels (Figure 6H). Colocalization analysis of more than six double-labeled cells resulted in similar values (data not shown).

FRET Analysis

The resolution of the light microscope does not allow determination of whether PAL directly interacts with C4H. This was addressed by a FRET approach. FRET is a quantum mechanical

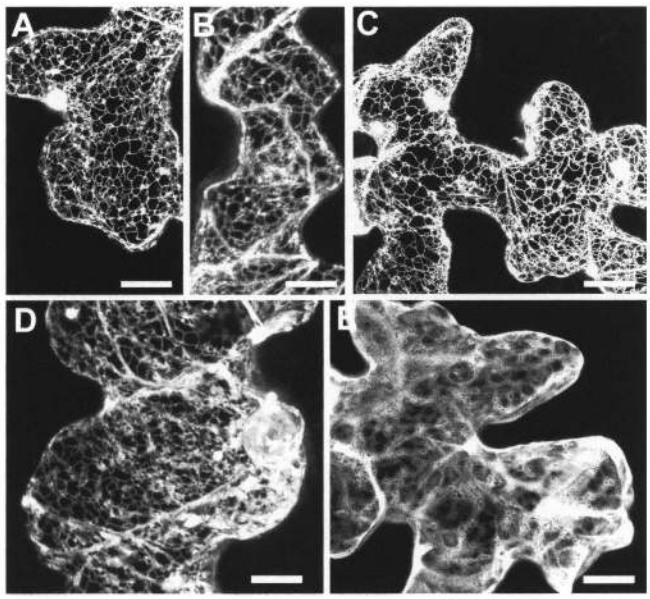

Figure 4. In Vivo Localization of PAL-eGFP Fusion Proteins in Leaf Epidermal Cells of Transgenic Tobacco Plants Expressing C4H-c-myc.

Transient expression of PAL1-eGFP **(A)** and PAL2-eGFP **(B)** fusion proteins in *C4H-c-myc*–expressing tobacco epidermal cells was achieved by bombardment of the corresponding expression constructs. Cells were also cobombarded with PAL1-eGFP and PAL2-pRTL2 **(C)** and PAL2-eGFP and PAL1-pRTL2 (**[D]** and **[E]**). The cell in **(D)** was observed 11 h after bombardment and after 15 h in **(E)**. Note the similar reticulate pattern of localization for PAL1-eGFP in **(A)** and PAL2-eGFP in **(B)** and loss of the reticulate localization of PAL2 in **(E)**. Bars = 20 μm in **(A)** to **(C)** and 10 μm in **(D)** and **(E)**.

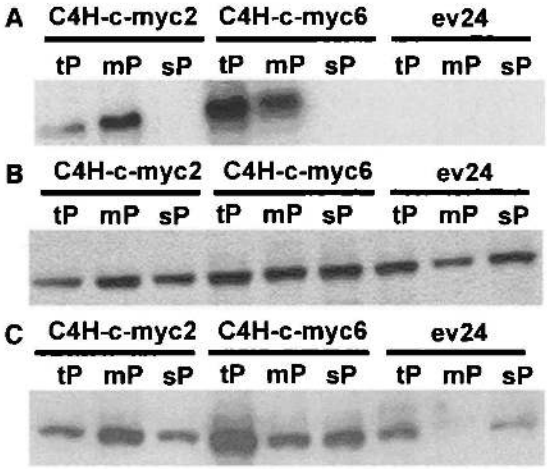

Figure 5. Subcellular Localization of PAL Isoforms and C4H in C4H-c-myc–Expressing Transgenic Tobacco.

Protein levels were measured by gel blot analysis in the total (tP), microsomal (mP; 130,000*g* pellet), and soluble (sP; 130,000*g* supernatant) fractions (15 μg protein/lane) from C4H-cmyc–expressing and empty-vector control lines.

(A) C-myc epitope-tagged tobacco C4H protein identified using anti-c-myc epitope antibody.

(B) Tobacco PAL1 protein detected with anti-(tobacco PAL1) serum.

(C) Tobacco PAL2 protein detected with anti-(tobacco PAL2) serum.

process that involves the transfer of energy between two closely positioned fluorophores (Day et al., 2001). This radiationless transfer of energy can only occur over a limited distance, making FRET a powerful tool for noninvasive monitoring of protein–protein interactions (Wu and Brand, 1994; Selvin, 1995). Because the emission spectrum of the donor fluorophore must overlap with the excitation spectrum of the acceptor for FRET to occur (Periasamy, 2001), Alexa Fluor-488 and cyanine 3 (Cy3) were used as the FRET pair. To minimize bleed-through, samples were scanned sequentially rather than simultaneously (Smallcombe, 2001).

Figure 7 shows representative images from FRET analysis of double-labeled tobacco protoplasts. Both PAL isoforms (donors) and C4H (acceptor) display the typical reticulate network characteristic of ER localization upon excitation with the appropriate laser line (488 nm for PAL and 568 nm for C4H; Figures 7A, 7B, 7E, and 7F). When the 488-nm line was used to excite the samples and acceptor (C4H) emission detected, the fluorescence pattern was similar to that of donor fluorescence (Figures 7C and 7G). This fluorescence, however, also contains contaminating signal from both donor cross talk and acceptor bleed-through (Elangovan et al., 2003). These contaminating signals were removed to obtain a corrected FRET image (Figures 7D and 7H), and energy transfer efficiency was calculated by ratioing the donor image in the presence and absence of the acceptor (Elangovan et al., 2003). The results of seven independent measurements of energy transfer efficiency for both PAL1:C4H and PAL2:C4H interactions gave values from 18 to 41%, indicating separation of the fluorophores by 71.6 to 86.9 Å.

The need to subtract contaminating signals in the above type of FRET analysis suggests that caution should be applied to the interpretation. An alternative approach to determining the extent of FRET is to monitor the dequenching of donor fluorescence after complete photobleaching of the acceptor chromophore (Vermeer et al., 2004). In this case, donor energy would not be transferred to the acceptor, and an increase in donor fluorescence intensity should result if donor and acceptor are tightly coupled. The data from a representative acceptor photobleaching experiment in tobacco protoplasts labeled with antibodies against PAL2 and c-myc (C4H) are shown in Figure 7I. The acceptor (C4H-Cy3) was bleached by continuously illuminating the samples with the 568-nm line of the krypton/argon laser, and the postbleach donor (Alexa Fluor) image was taken directly after bleaching Cy3. The pseudocolored images in Figure 7I represent the fluorescence intensities of protoplasts before and after acceptor photobleaching. The drastic reduction in the number of red and yellow pixels in the acceptor indicates the successful photobleaching (Figure 7I). However, from a comparison of the donor fluorescence intensity of postbleach and prebleach images, there appeared to be no increase of donor (Alexa Fluor-PAL2) fluorescence after bleaching of C4H-Cy3, indicating that energy transfer efficiency is low. This experiment was repeated for both PAL1-C4H and PAL2-C4H pairs, examining 12 to 15 cells from two independent antibody-labeling experiments; in each case the results were similar, with only one or two cells appearing to show a low increase in donor emission.

DISCUSSION

Differential Subcellular Localization of Tobacco PAL1 and PAL2

PAL is an operationally soluble enzyme that does not possess any obvious membrane anchor or membrane-spanning domains. Nevertheless, biochemical fractionation studies have suggested an association of PAL with ER membranes (Czichi and Kindl, 1975, 1977; Wagner and Hrazdina, 1984; Hrazdina and Wagner, 1985b). Cell fractionation, ultracentrifugation, and gel filtration experiments showed that PAL and the flavonoid pathway enzymes chalcone synthase and uridine diphosphate glucose flavonoid glucosyl transferase in buckwheat (*Fagopyrum esculentum*) were loosely associated with the cytoplasmic face of the ER (Hrazdina and Jensen, 1992). However, such biochemical approaches can be prone to artifacts arising from nonspecific associations. These data confirm our earlier report of differential subcellular localization of PAL1 (a significant percentage of which is microsomal) and PAL2 (cytosolic) in the wild-type tobacco (Rasmussen and Dixon, 1999) and extend the experimental approach to include in vivo analysis using GFP fusions and colocalization measurements using dual labeling and FRET. The exclusive ER localization of C4H has previously been shown in hybrid poplar (*Populus* spp) (Ro et al., 2001).

The intracellular localization of PAL forms determined by protein gel blot analysis was identical whether detection was by PAL isoform-specific antisera or relied on the use of transgenic plants in which the different PAL isoforms were tagged with different epitopes for detection by epitope-specific antisera. The fact that both approaches give the same results confirms the

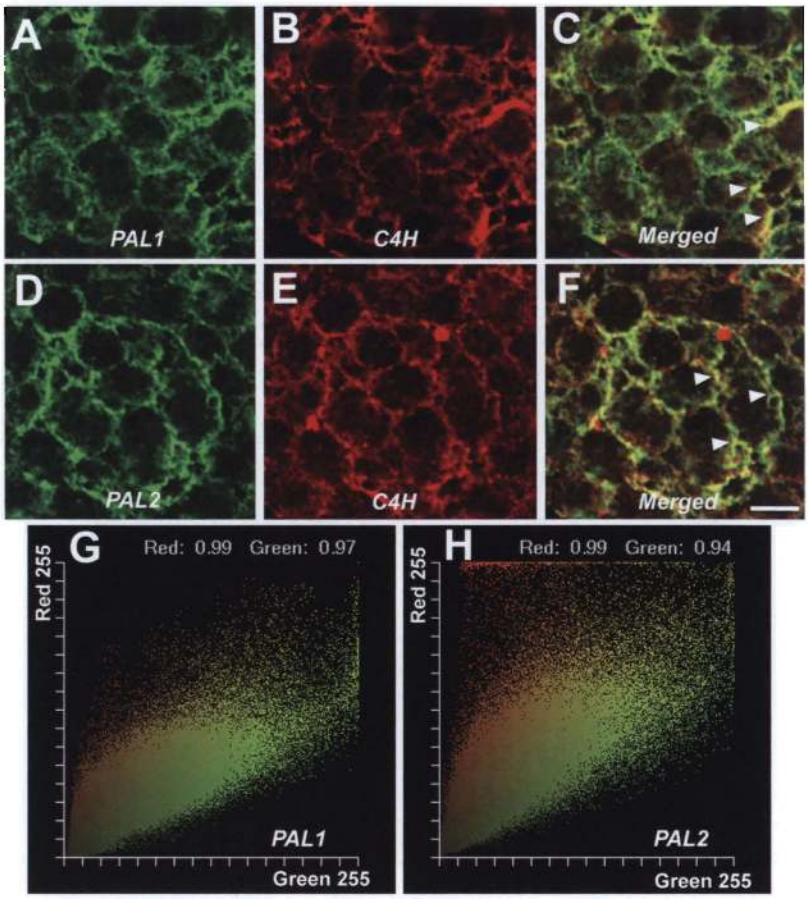

Figure 6. Colocalization of PAL and C4H in Leaf Protoplasts of C4H-c-myc–Expressing Tobacco.

The reticulate fluorescence pattern of the Alexa Fluor-488 reporting the location of PAL1 **(A)** and PAL2 **(D)** is highly similar to the pattern of Texas Red fluorescence reporting the location of C4H (**[B]** and **[E]**). Colocalization of PAL1 with C4H **(C)** and PAL2 with C4H **(F)** is shown in the merged images. Colocalization is indicated by yellow where the green and red colors are superimposed. Arrowheads indicate typical colocalizations. The green (**[A]** and **[D]**) and red (**[B]** and **[E]**) components are depicted as two-dimensional scattergrams for PAL1-C4H **(G)** and PAL2-C4H **(H)**. High colocalization coefficients were obtained for the green and red components for both interactions (**[G]** and **[H]**). Bars = 10 μm for all panels.

differential subcellular localization of tobacco PAL1 and PAL2 and also shows that epitope-tagged PAL forms expressed transgenically localize to the same subcellular fractions as the wild-type forms in nontransgenic cells. The apparently stronger ER localization of PAL1-eGFP in C4H-overexpressing plants compared with the wild-type plants was not reflected by the protein gel blot analyses, which indicated recovery of a significant proportion of PAL1 in the soluble fraction from both the wild type and C4H-c-myc transgenics. This is consistent with a loose association between PAL and its membrane-associated target, such that, in spite of strong membrane localization as viewed by confocal microscopy in live cells, cellular extraction results in disruption of the complex.

PAL Colocalizes with C4H in Tobacco Microsomes

It has been proposed that membrane-anchored cytochrome P450 enzymes might function to nucleate complexes of metabolic enzyme to the outer surface of the ER (Hrazdina and Jensen, 1992; Chapple, 1998). This concept has been indirectly addressed by studies on the cyanogenic glucoside pathway in *Sorghum bicolor*, which can be reconstituted in vitro using two recombinant P450s, CYP79 and CYP71E1 (Bak et al., 1998), the monolignol pathway in microsomal preparations from lignifying stems of alfalfa (*Medicago sativa*) containing *O*-methyltransferase and coniferaldehyde 5-hydroxylase cytochrome P450 (Guo et al., 2002), and the entry point into isoflavonoid biosynthesis, in which an operationally soluble *O*-methyltransferase localizes to endomembranes containing the isoflavonone synthase cytochrome P450 after elicitation of the isoflavonoid pathway (Liu and Dixon, 2001). However, in none of these studies has it been directly shown that the P450 itself is the target for localizing the operationally soluble partner enzyme to the endomembrane system.

We have now addressed whether the tobacco PAL1 does indeed directly colocalize with the C4H cytochrome P450, using both colocalization software for analysis of confocal images and the more sensitive FRET technique. The rationale for performing

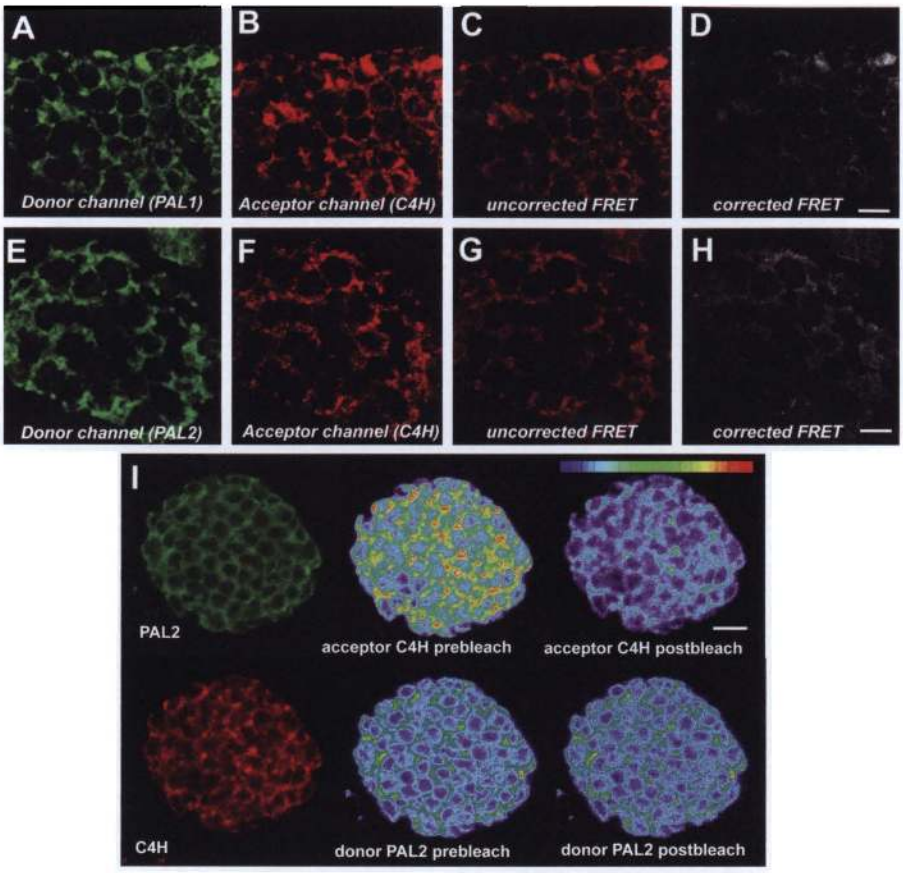

Figure 7. FRET Microscopy in Tobacco Protoplasts Double Labeled with Alexa Fluor-488 and Cy3.

Precision FRET (pFRET) data analysis was conducted according to the methods of Elangovan et al. (2003). Single optical sections from the confocal microscope were acquired for FRET analysis using the same aperture settings, gain, and laser intensity. Double-labeled protoplasts are shown for PAL1-C4H (**[A]** to **[D]**) and PAL2-C4H (**[E]** to **[H]**). Donor excitation/donor emission and acceptor excitation/acceptor emission shows the reticulate fluorescence pattern of PAL (**[A]** and **[E]**) and C4H (**[B]** and **[F]**). Donor excitation/acceptor emission shows a fluorescence signal that includes FRET, donor cross talk, and acceptor bleed-through contaminants (uncorrected FRET) (**[C]** and **[G]**). The image after removal of donor cross talk and acceptor bleed-through represents actual FRET signal (**[D]** and **[H]**). Confocal fluorescence images of tobacco protoplasts before and after acceptor photobleaching **(I)**. Fluorescence intensities have been pseudocolored according to the inset scale, with red pixels indicating intense fluorescence and blue pixels indicating weak fluorescence. Bars = 10 μm for all panels.

the FRET analysis was to determine whether the PAL isoforms directly interact with C4H in the endomembrane system rather than simply colocalizing. In FRET, the efficiency of energy transfer is dependent on the physical distance between the donor and acceptor fluorophores, which have to be within 10 to 100 Å from each other for FRET to occur (Gadella et al., 1999). Detection of FRET has been used previously to determine protein–protein interactions using different spectral variants of GFP in living plant cells (Mas et al., 2000; Immink et al., 2002; Kato et al., 2002; Vermeer et al., 2004) or by indirect immunofluorescence in fixed plant material (Durso et al., 1996). In our study, we detected FRET signals in fixed tobacco protoplasts using a recently developed FRET data analysis algorithm that allowed us to remove spectral bleed-through and correct for variation in fluorophore concentration level (Elangovan et al., 2003). Our FRET analysis estimates that PAL and C4H are separated by a distance of ~80 Å on the surface of the ER, close to the theoretical limit for observing FRET. FRET measurements in animal systems show estimated distances ranging from 28 Å in protein dimers (Levi et al., 2000) to 90 Å between the active site of a membrane bound protein and the phospholipid surface of the membrane (Yegneswaran et al., 1997). Our estimated distance of 80 Å between PAL and C4H could therefore be typical of weak protein–protein interactions at the surface of the membrane. To validate the FRET results obtained using the pFRET algorithm, we employed acceptor photobleaching experiments on labeled protoplasts. Acceptor photobleaching FRET microscopy is a more straightforward approach for performing FRET. By bleaching the acceptor chromophore with a high-power laser beam, the acceptor can no longer accept energy from the donor; therefore, this should result in an increase in donor fluorescence. However, in our experiments, bleaching the acceptor did not result in any substantial increase in donor fluorescence (Figure 7I). Our inability to show dequenching of the donor fluorescence

after acceptor photobleaching could be indicative of low physical interaction between PAL and C4H, and the distance estimated using pFRET software is perhaps an overestimate of the actual distance between PAL and C4H. Alternatively, our inability to show increased donor fluorescence after acceptor photobleaching could be because of other reasons. First, the acceptor chromophore Cy3 is quite stable, and it was impossible to completely bleach Cy3 despite continuous laser illumination. The typical FRET pair for acceptor photobleaching studies in fixed cells is Cy3 (donor)-Cy5 (acceptor) because Cy5 can be readily photobleached (Kenworthy and Edidin, 1998). Incomplete photobleaching of the acceptor could result in continued dequenching of the donor. We attempted using Cy5 as the acceptor dye. However, the emission of chloroplasts from the labeled cells made it difficult to assess the efficiency of photobleaching. Second, it is possible that the donor chromophore was also bleached by intense illumination from the 568-nm laser source; therefore, any increase in fluorescence emission because of FRET is masked. This scenario is likely because we observed a reduction in donor fluorescence in some cells after acceptor photobleaching (data not shown). Finally, the presence of a significant proportion of the donor in the soluble fraction, and, thus, not close to the acceptor, reduces the relative proportion of donor that can participate in FRET. Nevertheless, the fact that PAL2 also exhibits ER localization in cells in which C4H is overexpressed and that increasing expression of PAL1 can displace PAL2 from its membrane localization not only points to C4H or another protein associated with C4H as a potential membrane anchor for PAL, but also indicates that different PAL forms associate with C4H, or other potential proteins in the complex, with differing affinities.

In the absence of antibodies specific for tobacco C4H, it was not possible to demonstrate the lack of FRET between PAL2 and C4H in plants with the wild-type C4H levels. This would be expected, however, based on the clear cytosolic localization of PAL2-eGFP in such plants (Figures 2 and 3). Future studies will employ fusions of the PAL isoforms and C4H with the other spectral variants of GFP (Mas et al., 2000; Immink et al., 2002; Kato et al., 2002; Vermeer et al., 2004) in stably transformed plants to gain a better understanding of the in vivo interaction between these two components of the phenylpropanoid pathway. The membrane localization of PAL2 in plants overexpressing C4H points to the need for caution in interpreting any study on protein colocalization when overexpression is necessary to introduce a labeled form of the protein. This caution also extends to transient assays, as performed here, in which expression level is not tightly controlled, although examination of multiple bombarded cells, as we have done, provides good confidence that the effects are not simply the result of aberrant localization of excessively expressed proteins.

Consequences of PAL Localization for Metabolic Channeling in Phenylpropanoid Biosynthesis

It is becoming increasingly apparent that consecutive reactions of natural product biosynthesis may be organized as complexes, known as metabolic compartments or metabolons, through which pathway intermediates can be channeled without equilibration with free cytoplasmic pools (Stafford, 1974; Hrazdina and Wagner, 1985b; Srere, 1987; Hrazdina and Jensen, 1992; Rasmussen and Dixon, 1999; Saslowsky and Winkel-Shirley, 2001; Winkel, 2004). Channeling of cinnamic acid between PAL and C4H in vivo was demonstrated in tobacco cell suspension cultures fed with ^{3}H-L-Phe; a significant proportion of the ^{3}H-*trans*-cinnamic acid formed from ^{3}H-L-Phe did not equilibrate with exogenously supplied [^{14}C]-*trans*-cinnamic acid and may therefore be rapidly channeled through the C4H reaction to 4-coumaric acid. This channeling was confirmed in vitro in isolated microsomes from tobacco stems or cell suspension cultures (Rasmussen and Dixon, 1999). By contrast, the same double-labeling approach failed to indicate channeling of endogenously formed cinnamate in yeast (*Saccharomyces cerevisiae*) expressing recombinant poplar PAL and C4H (Ro and Douglas, 2004). These studies did not examine whether PAL was colocalized with C4H on the yeast endomembranes.

These results explain metabolic channeling of cinnamic acid in tobacco as resulting from colocalization of a portion of the PAL1 pool with C4H. Our estimates indicate, however, that this channeling does not result from a close, tight physical interaction between the two enzymes. Cinnamic acid itself is a hydrophobic molecule, and it is possible that it is delivered from PAL1 to C4H by movement within the outer face of the ER.

Immunolocalization experiments do not distinguish between active and inactive enzymes; PAL is subject to posttranslational modifications that may affect catalytic activity (Bolwell et al., 1985; Bolwell, 1992; Allwood et al., 1999), and we do not know at present whether the specific activities of the soluble and membrane-associated forms of PAL are the same. We postulate that the fraction of PAL1 associated with the ER is catalytically active and is responsible for channeling of cinnamic acid.

Presumably, cinnamic acid produced by PAL2 is not closely channeled through C4H in cells in which PAL1 protein predominates, but rather reaches C4H by diffusion through the cytosol. Although it has been reported that tobacco PAL1 and PAL2 have similar developmental and tissue-specific expression patterns (Fukasawa-Akada et al., 1996), more work is necessary to determine whether the ratios of PAL1 to PAL2 differ during development or in response to environmental stimuli, and, if so, whether this itself has metabolic consequences independent of the overall level of PAL activity.

Differential subcellular distributions of cinnamic acid arising from the activities of differentially localized PAL isoforms could help partition phenylpropanoid biosynthesis into different branch pathways. For example, some pathways of phenylpropanoid biosynthesis can bypass the C4H reaction. These include 2-hydroxylation of cinnamic acid by chloroplastic cinnamate 2-hydroxylase (Gestetner and Conn, 1974), glucosylation of cinnamic acid by UDP glucose:*trans*-cinnamic acid glucosyltransferase (Shimizu and Kojima, 1984; Edwards et al., 1990), and the biosynthesis of B-ring deoxy-flavonoids such as baicalein via a coumarate CoA ligase isoform that is active with cinnamic acid (Liu et al., 1995). Lignin, flavonoid, and chlorogenic acid biosynthesis in tobacco might operate through the channeled PAL isoform. In addition, associations between PAL and C4H might help to reduce the size of the cellular cinnamate pool and thereby reduce potential feedback inhibition of PAL by

cinnamate (Noe et al., 1980). Downregulation of C4H leads to a reduction in PAL activity in transgenic tobacco, possibly via feedback by cinnamate (Blount et al., 2000).

Because of metabolic channeling associated with membrane-associated complexes harboring specific isoforms of a particular enzyme, changes in metabolism resulting from overexpression of one enzyme isoform may not always simply reflect a quantitative increase in enzyme activity or a qualitative alteration in isoform pattern with associated kinetic consequences. Alterations in subcellular localization of enzyme isoforms might provide an extra and unsuspected level of metabolic regulation. Furthermore, a requirement for precise subcellular organization of enzymes of phenylpropanoid biosynthesis would affect genetic engineering strategies for overproduction or elimination of end products if the product of the introduced transgene was incorrectly localized or perturbed the localization of an endogenous enzyme.

METHODS

Plant Material

Tobacco (*Nicotiana tabacum* cv Xanthi-nc) plants were transformed with epitope-tagged tobacco PAL1, PAL2, or C4H. PAL1-HA and HA-PAL1 (HA peptide YPYDVPDYA from human influenza hemagglutinin), PAL2-VSV-G and VSV-G-PAL2 (VSG-G peptide YTDIEMNRLGK from vesicular stomatitis virus glycoprotein), and C4H-c-myc (human c-myc epitope EQKLISEEDL) (Roche Applied Science, Indianapolis, IN) were cloned into pBI121 and tobacco leaf discs transfected with *Agrobacterium tumefaciens* harboring the constructs. Transgenic plants were regenerated (Horsch et al., 1988) and grown under greenhouse conditions (27°C day, 18°C night). Tissue samples were frozen at −80°C until used. Young leaves for transient expression or colocalization experiments were freshly harvested.

DNA Gel Blot Analysis

Isolated genomic DNA from C4H-c-myc2, C4H-c-myc6, or ev24 (10 μg) was digested using 30 units of *Bam*HI, *Eco*RI, or *Xba*I. Genomic DNA from P1ct17, P1ct18, and ev24 genomic DNA (10 μg) was digested with 30 units of *Sac*I, *Xba*I, or *Xho*I. Genomic DNA (10 μg) from P2ct3, P2ct5, and ev24 was digested with 30 units of *Eco*RI, *Xba*I, or *Xho*I. Products were run on a 0.8% agarose gel and transferred onto Hybond N · membranes (Amersham, Little Chalfont, UK) according to the manufacturer's instructions. Membranes were prehybridized for 2 h in hybridization solution (Church and Gilbert, 1984). Radiolabeled DNA probes of 1.5 kb C4H or 2.1 kb PAL1 or PAL2 sequences were generated by random priming using the High Prime labeling kit (Roche Applied Science) according to the manufacturer's instructions. The denatured probe was added to the prehybridization solution, and membranes were hybridized overnight at 65°C. Two washes in 2× SSC (1× SSC is 0.15 M NaCl and 0.015 M sodium citrate) and 0.1% SDS at room temperature, and two washes in 0.1× SSC and 0.1% SDS at 65°C were performed to remove nonspecific hybridization. Membranes were then exposed to PhosphorImager screens (Molecular Dynamics, Sunnyvale, CA) and scanned using a Typhoon 8600 scanner (Amersham).

PAL and C4H Assays

PAL (cytosolic) and C4H (microsomal) activities were assayed in extracts of leaf material as described previously (Edwards and Kessmann, 1992) except that for PAL assay 50 μL of crude enzyme extract was used in a total volume of 1.0 mL, and the absorbance of cinnamic acid was determined in 100-μL aliquots as a function of time in a UV2401PC spectrophotometer (Shimadzu, Columbia, MD) using a 16-sample microcell. All enzyme assays were performed in triplicate. Protein concentrations were determined by the Bradford procedure (Bradford, 1976).

Antibodies

Synthetic peptides VRDKSANG (positions 69 to 76, tobacco PAL1) and VAQNGHQEMDFCMKV (positions 4 to 18, tobacco PAL2) were coupled to keyhole limpet hemocyanin, and antibodies to discriminate between PAL1 and PAL2 were raised in rabbits (Genosys Biotechnologies, The Woodlands, TX). Mouse monoclonal antibodies conjugated with peroxidase-conjugated anti-HA, anti-VSV-G, or anti-c-myc were purchased from Roche Applied Science.

Protein Gel Blot Analysis

Total, soluble, and microsomal protein extracts (10 to 20 μg) were run on 8 to 10% precast Tris-Glycine gels (Novex, San Diego, CA) in a Novex Xcell II mini cell electrophoresis system at 50 V for 1 h followed by 80 V for 2 h along with kaleidoscope prestained molecular weight standards (Bio-Rad, Hercules, CA). Proteins were transferred to a polyvinylidene difluoride nitrocellulose membrane (Immobilon-P; Millipore, Burlington, MA) at 25 V for 2 to 3 h. Membranes were blocked overnight in PBS containing 5% Carnation dried milk (Carnation, Glendale, CA), treated with primary antibody at 1:1000 dilution for 2 h and then with 1:10,000 dilution in PBST of secondary antibody (anti-rabbit IgG coupled to horseradish peroxidase; Bio-Rad). Bands were visualized on Kodak film by chemiluminescence assay (ECL; Amersham). Incubation of blots with horseradish peroxidase–conjugated anti-HA, anti-VSV-G, or anti-c-myc was performed following the manufacturer's instructions.

Cloning Procedures and Plasmid Construction

All DNA manipulations, including PCR, restriction digestion, agarose gel electrophoresis, ligation, and transformation into *Escherichia coli* DH5α or *A. tumefaciens* LBA4404, were performed by standard procedures (Sambrook et al., 1989).

PAL1 is defined as the protein encoded by the *PAL1* gene described by Fukasawa-Akada et al. (1996), and PAL2 as the product of the *PAL11* gene described by Nagai et al. (1994) (Figure 1A). To make PAL1 and PAL2 C-terminal fusion proteins with eGFP (Clontech, Palo Alto, CA), the PAL coding regions were amplified by PCR with the following primers: PAL1 forward 5′-CCCGCTCGAGATGGCATCAAATGGTCATGTTAATGG-3′ and reverse 5′-CTCCCCGCGGACAGATAGGAAGAGGAGCACC-3′; PAL2 forward 5′-CCCGCTCGAGATGGCTGGTGTTGCACAAAATG-3′ and reverse 5′-CTCCCCGCGGACAGATTGGAAGAGGTGCACC-3′, containing *Xho*I and *Sac*II sites (underlined). PCR products were recovered, gel purified, and double digested with *Xho*I and *Sac*II, and the PAL open reading frames were inserted into the multiple-cloning site of the shuttle vector p-EGFP-1 (Clontech). Chimeric *PAL1-eGFP* and *PAL2-eGFP* genes were digested with *Xho*I and *Xba*I and inserted into the corresponding sites of pRTL2 (Restrepo et al., 1990) under control of a double 35S promoter of *Cauliflower mosaic virus*. *eGFP* was excised from pEGFP-1 by digestion with *Xho*I and *Xba*I and inserted into pRTL2 to make pRTL2-eGFP-1. The C4H-MA C-terminal eGFP fusion was made by PCR amplifying the C4H-MA with forward 5′-TCCCCCCGGGATGGATCTTCTCTTACTAGAG-3′ and reverse 5′-GCGGGATCCTCAACGCTTTGAACGAAGTTTAGA-3′ primers containing *Xma*I and *Bam*HI sites (underlined) and cloning the PCR products into pRTL2-eGFP-1. All PCR-amplified products were sequenced to confirm the absence of mutations.

Particle Bombardment and Confocal Microscopy

Plasmid DNA (~5 μg) harboring eGFP fusion genes was mixed with 1.0 μm gold particles for biolistic bombardment as described previously (Liu and Dixon, 2001). Young tobacco leaves were excised and placed on moist filter paper in Petri dishes. Particle bombardment (Bio-Rad 1000/He particle delivery system), cellular imaging using a Bio-Rad 1024ES confocal imaging system attached to a Zeiss Axioskop microscope (Carl Zeiss, Thornwood, NY), and collection and processing of serial optical images were performed as described previously (Liu and Dixon, 2001).

PAL and C4H Colocalization Studies

Colocalization of PAL and C4H was studied in leaf palisade protoplasts of C4H-c-myc–expressing tobacco plants. Protoplasts were prepared according to the method of Kubo and Takanami (1979), collected by centrifugation, and fixed for immunolabeling. Fixation was for 30 min in 3% (v/v) formaldehyde in PEM (50 mM Pipes, 10 mM EGTA, and 5 mM $MgSO_4$) buffer, pH 6.9, and 5% dimethyl sulfoxide (v/v). Fixed protoplasts were washed in PEM buffer, gently layered onto 22 × 22-mm cover slips using a thin film of agar, and blocked with 3% (w/v) BSA in PEM buffer for 1 h. Primary antibodies (rabbit anti-PAL1 or anti-PAL2 and mouse anti-c-myc) diluted 1:200 in 1% (w/v) BSA in PEM buffer were applied overnight in a humid chamber. After extensive washing in PEM buffer, protoplasts were exposed to secondary antibodies (goat anti-rabbit IgG conjugated to Alexa Fluor-488 [Molecular Probes, Eugene, OR] and donkey anti-mouse IgG conjugated to Cy3 [Jackson ImmunoResearch, West Grove, PA]) for 2 to 4 h, washed several times in PEM buffer, and mounted in 20% Mowiol 4-88 (Calbiochem, La Jolla, CA) containing phenylenediamine (0.1%) in PBS, pH 8.5.

Protoplasts were imaged with a Bio-Rad 1024 ES confocal microscope. Single optical sections were collected and Kalman averaged three times. Alexa Fluor was detected by exciting the samples with the 488-nm laser line and measuring emission at 522 nm, whereas Cy3 was excited using the 568-nm line and emission detected at 585 nm. The captured images were pseudocolored green or red and digitally overlaid to visualize colocalization. Collected images were processed using Adobe Photoshop 5.0L.E (Adobe Systems, Mountain View, CA).

FRET Analysis of PAL/C4H Colocalization in Fixed Protoplasts

Protoplasts were either double labeled as described above or single labeled with either the donor (Alexa Fluor-488 for PAL) or acceptor (Cy3 for C4H). The single-labeled samples were used to determine spectral bleed-through levels. Images of single-labeled donor or acceptor and double-labeled donor plus acceptor were collected at the donor excitation wavelength (488 nm) or acceptor excitation wavelength (568 nm). Seven single-scanned images were collected using the same conditions of laser intensity, pinhole size, and gain levels. Images for precision FRET were processed and analyzed using the software and methods of Elangovan et al. (2003).

To perform the acceptor photobleaching experiments, protoplasts double labeled with Alexa Fluor-488 and Cy3 were used. An initial image of Alexa Fluor and Cy3 was obtained using 488-nm excitation and 568-nm excitation, respectively. Cy3 was photobleached by continuously scanning a field of protoplasts with the 568-nm laser line set at 100% intensity for 1 min. An image of Alexa Fluor and Cy3 was then collected using the respective excitation lines. Data were collected from three different fields from three independent slide preparations. Fluorescence intensities were pseudocolored using Metamorph 5.0 image processing (Universal Imaging, West Chester, PA).

ACKNOWLEDGMENTS

We thank Rujin Chen and Xin-Shun Ding (Noble Foundation) for critical reading of the manuscript and Ammasi Periasamy (University of Virginia) for precision FRET software. This work was supported by the Samuel Roberts Noble Foundation.

Received May 25, 2004; accepted August 22, 2004.

REFERENCES

Allwood, E.G., Davies, D.R., Gerrish, C., Ellis, B.E., and Bolwell, G.P. (1999). Phosphorylation of phenylalanine ammonia-lyase: Evidence for a novel protein kinase and identification of the phosphorylated residue. FEBS Lett. **457,** 47–52.

Bak, S., Kahn, R.A., Nielsen, H.L., Moller, B.L., and Halkier, B.A. (1998). Cloning of three A-type cytochromes P450, CYP71E1, CYP98, and CYP99 from *Sorghum bicolor* (L.) Moench by a PCR approach and identification by expression in *Escherichia coli* of CYP71E1 as a multifunctional cytochrome P450 in the biosynthesis of the cyanogenic glucoside dhurrin. Plant Mol. Biol. **36,** 393–405.

Blount, J.W., Korth, K.L., Masoud, S.A., Rasmussen, S., Lamb, C., and Dixon, R.A. (2000). Altering expression of cinnamic acid 4-hydroxylase in transgenic plants provides evidence for a feedback loop at the entry point into the phenylpropanoid pathway. Plant Physiol. **122,** 107–116.

Bolwell, G.P. (1992). A role for phosphorylation in the down-regulation of phenylalanine ammonia-lyase in suspension-cultured cells of french bean. Phytochemistry **31,** 4081–4086.

Bolwell, G.P., Sap, J., Cramer, C.L., Schuch, W., Lamb, C.J., and Dixon, R.A. (1985). L-Phenylalanine ammonia-lyase from *Phaseolus vulgaris*: Partial degradation of enzyme subunits *in vitro* and *in vivo*. Biochim. Biophys. Acta **881,** 210–221.

Bradford, M.M. (1976). A rapid and sensitive method for the quantitation of microgram quantities of protein utilizing the principle of protein-dye binding. Anal. Biochem. **72,** 248–254.

Chapple, C. (1998). Molecular-genetic analysis of plant cytochrome P450-dependent monooxygenases. Annu. Rev. Plant Physiol. Plant Mol. Biol. **49,** 311–343.

Church, G.H., and Gilbert, W. (1984). Genomic sequencing. Proc. Natl. Acad. Sci. USA **81,** 65–71.

Cramer, C.L., Edwards, K., Dron, M., Liang, X., Dildine, S.L., Bolwell, G.P., Dixon, R.A., Lamb, C.J., and Schuch, W. (1989). Phenylalanine ammonia-lyase gene organization and structure. Plant Mol. Biol. **12,** 367–383.

Czichi, U., and Kindl, H. (1975). Formation of *p*-coumaric acid and *o*-coumaric acid from L-phenylalanine by microsomal membrane fractions from potato: Evidence of membrane-bound enzyme complexes. Planta **125,** 115–125.

Czichi, U., and Kindl, H. (1977). Phenylalanine ammonia-lyase and cinnamic acid hydroxylase as assembled consecutive enzymes on microsomal membranes of cucumber cotyledons: Cooperation and subcellular distribution. Planta **134,** 133–143.

Day, R., Periasamy, A., and Schaufele, F. (2001). Fluorescence resonance energy transfer microscopy of localized protein interactions in the living cell nucleus. Methods **25,** 4–18.

Dixon, R.A., Achnine, L., Kota, P., Liu, C.-J., Reddy, M.S., and Wang, L. (2002). The phenylpropanoid pathway and plant defense: A genomics perspective. Mol. Plant Pathol. **3,** 371–390.

Dixon, R.A., Canovas, P., Guo, Z.-J., He, X.-Z., Lamb, C., and

McAlister, F. (1999). Molecular controls for isoflavonoid biosynthesis in relation to plant and human health. Recent Adv. Phytochem. **33,** 133–160.

Dixon, R.A., and Sumner, L.W. (2003). Legume natural products. Understanding and manipulating complex pathways for human and animal health. Plant Physiol. **131,** 878–885.

Durso, N.A., Leslie, J.D., and Cyr, R.J. (1996). In situ immunocytochemical evidence that a homolog of protein translation elongation factor EF-1 alpha is associated with microtubules in carrot cells. Protoplasma **190,** 141–150.

Edwards, R., and Kessmann, H. (1992). Isoflavonoid phytoalexins and their biosynthetic enzymes. In Molecular Plant Pathology: A Practical Approach, S.J. Gurr, M.J. McPherson, and D.J. Bowles, eds (Oxford: IRL Press), pp. 45–62.

Edwards, R., Mavandad, M., and Dixon, R.A. (1990). Metabolic fate of cinnamic acid in elicitor-treated cell suspension cultures of *Phaseolus vulgaris*. Phytochemistry **29,** 1867–1873.

Elangovan, M., Wallrabe, H., Chen, Y., Day, R., Barroso, M., and Periasamy, A. (2003). Characterization of one- and two-photon excitation fluorescence resonance energy transfer microscopy. Methods **29,** 58–73.

Frigerio, L., Pastres, A., Prada, A., and Vitale, A. (2001). Influence of KDEL on the fate of trimeric or assembly-defective phaseolin: Selective use of an alternative route to vacuoles. Plant Cell **13,** 1109–1126.

Fukasawa-Akada, T., Kung, S., and Watson, J.C. (1996). Phenylalanine ammonia-lyase gene structure, expression, and evolution in *Nicotiana*. Plant Mol. Biol. **30,** 711–722.

Gadella, T.W.J., van der Krogt, G.N.M., and Bisseling, T. (1999). GFP-based FRET microscopy in living plant cells. Trends Plant Sci. **4,** 287–291.

Gestetner, B., and Conn, E.E. (1974). The 2-hydroxylation of trans-cinnamic acid by chloroplasts from *Melilotus alba* Desr. Arch. Biochem. Biophys. **163,** 617–624.

Guo, D., Chen, F., and Dixon, R.A. (2002). Monolignol biosynthesis in microsomal preparations from lignifying stems of alfalfa (*Medicago sativa* L.). Phytochemistry **61,** 657–667.

Haseloff, J., Siemering, K.R., Prasher, D.C., and Hodges, S. (1997). Removal of a cryptic intron and subcellular localization of green fluorescent protein are required to mark transgenic Arabidopsis brightly. Proc. Natl. Acad. Sci. USA **94,** 2122–2127.

Heinlein, M., Padgett, H.S., Gens, J.S., Pickard, B.G., Casper, S.J., Epel, B.L., and Beachy, R.N. (1998). Changing patterns of localization of the tobacco mosaic virus movement protein and replicase to the endoplasmic reticulum and microtubules during infection. Plant Cell **10,** 1107–1120.

Horsch, R.B., Fry, J., Hoffmann, N., Neidermeyer, J., Rogers, S.G., and Fraley, R.T. (1988). Leaf disc transformation. In Plant Molecular Biology Manual, S.P. Gelvin, R.A. Schilperoort, and D.P.S. Verma, eds (Dordrecht: Kluwer Academic Publishers), pp. 1–9.

Hrazdina, G., and Jensen, R.A. (1992). Spatial organization of enzymes in plant metabolic pathways. Annu. Rev. Plant Physiol. Plant Mol. Biol. **43,** 241–267.

Hrazdina, G., and Wagner, G.J. (1985a). Metabolic pathways as enzyme complexes: Evidence for the synthesis of phenylpropanoids and flavonoids on membrane associated enzyme complexes. Arch. Biochem. Biophys. **237,** 88–100.

Hrazdina, G., and Wagner, G.J. (1985b). Compartmentation of plant phenolic compounds: Sites of synthesis and accumulation. Annu. Proc. Phytochem. Soc. Europe **25,** 119–133.

Immink, R.G.H., Gadella, T.W.J., Ferrario, S., Busscher, M., and Angenent, G.C. (2002). Analysis of MADS box protein-protein interactions in living plant cells. Proc. Natl. Acad. Sci. USA **99,** 2416–2421.

Kato, N., Pontier, D., and Lam, E. (2002). Spectral profiling for simultaneous observation of four distinct fluorescent proteins and detection of protein-protein interaction via fluorescence resonance energy transfer in tobacco leaf nuclei. Plant Physiol. **129,** 931–942.

Kenworthy, A.K., and Edidin, M. (1998). Distribution of a glycosylphosphatidylinositol-anchored protein at the apical surface of MDCK cells examined at a resolution of <100Å using fluorescence resonance energy transfer. J. Cell Biol. **142,** 69–84.

Kubo, S., and Takanami, Y. (1979). Infection of tobacco mesophyll protoplasts with tobacco necrotic dwarf virus, a phloem-limited virus. J. Gen. Virol. **42,** 387–398.

Levi, V., Rossi, J.P.F.C., Castello, P.R., and Flecha, F.L.G. (2000). Oligomerization of the plasma membrane calcium pump involves two regions with differing thermal stability. FEBS Lett. **483,** 99–103.

Liu, C.-J., and Dixon, R.A. (2001). Elicitor-induced association of isoflavone O-methyltransferase with endomembranes prevents formation and 7-O-methylation of daidzein during isoflavonoid phytoalexin biosynthesis. Plant Cell **13,** 2643–2658.

Liu, Q., Seradge, E., Bonness, M.S., Liu, M., Mabry, T.J., and Dixon, R.A. (1995). Enzymes of B-ring-deoxy flavonoid biosynthesis in elicited cell cultures of "old man" cactus (*Cephalocereus senilis*). Arch. Biochem. Biophys. **321,** 397–404.

Manders, E., Verbeek, F., and Aten, J. (1993). Measurement of co-localization of objects in dual-colour confocal images. J. Microsc. **169,** 375–382.

Mas, P., Devlin, P.F., Panda, S., and Kay, S.A. (2000). Functional interaction of phytochrome B and cryptochrome 2. Nature **408,** 207–211.

Nagai, N., Kitauchi, F., Shimosaka, M., and Okazaki, M. (1994). Cloning and sequencing of a full-length cDNA coding for phenylalanine ammonia-lyase from tobacco cell culture. Plant Physiol. **104,** 1091–1092.

Noe, W., Langebartels, C., and Seitz, H.U. (1980). Anthocyanin accumulation and PAL activity in a suspension culture of *Daucus carota* L. Inhibition by L-α-aminooxy-β-phenylpropionic acid and *t*-cinnamic acid. Planta **149,** 283–287.

Pellegrini, L., Rohfritsch, O., Fritig, B., and Legrand, M. (1994). Phenylalanine ammonia-lyase in tobacco. Molecular cloning and gene expression during the hypersensitive reaction to tobacco mosaic virus and the response to a fungal elicitor. Plant Physiol. **106,** 877–886.

Periasamy, A. (2001). Fluorescence energy transfer microscopy: A mini review. J. Biomed. Opt. **6,** 287–291.

Rasmussen, S., and Dixon, R.A. (1999). Transgene-mediated and elicitor-induced perturbation of metabolic channeling at the entry point into the phenylpropanoid pathway. Plant Cell **11,** 1537–1551.

Restrepo, M.A., Freed, D.D., and Carrington, J.C. (1990). Nuclear transport of plant polyviral proteins. Plant Cell **10,** 987–998.

Ro, D.K., and Douglas, C.J. (2004). Reconstitution of the entry point of plant phenylpropanoid metabolism in yeast (*Saccharomyces cerevisiae*). J. Biol. Chem. **279,** 2600–2607.

Ro, D.K., Mah, N., Ellis, B.E., and Douglas, C.J. (2001). Functional characterization and subcellular localization of poplar (*Populus trichocarpa* × *Populus deltoides*) cinnamate 4-hydroxylase. Plant Physiol. **126,** 317–329.

Sambrook, J., Fritsch, E.F., and Maniatis, T. (1989). Molecular Cloning: A Laboratory Manual. (Cold Spring Harbor, NY: Cold Spring Harbor Laboratory Press).

Saslowsky, D., and Winkel-Shirley, B. (2001). Localization of flavonoid enzymes in Arabidopsis roots. Plant J. **27,** 37–48.

Selvin, P.R. (1995). Fluorescence resonance energy transfer. Methods Enzymol. **246,** 300–334.

Shimizu, T., and Kojima, M. (1984). Partial purification and characterization of UDPG:*t*-cinnamate glucosyltransferase in the root of sweet potato, *Ipomoea batatas* Lam. J. Biochem. **95,** 205–212.

Smallcombe, A. (2001). Multicolor imaging: The important question of co-localization. Biotechniques **30,** 1240–1246.

Srere, P.A. (1987). Complexes of sequential metabolic enzymes. Annu. Rev. Biochem. **56,** 89–124.

Stafford, H.A. (1974). Possible multienzyme complexes regulating the formation of C_6-C_3 phenolic compounds and lignins in higher plants. Recent Adv. Phytochem. **8,** 53–79.

Vermeer, J.E.M., Munster, E.B.V., Vischer, N.O., and Gadella, T.W.J. (2004). Probing plasma membrane microdomains in cowpea protoplasts using lipidated GFP fusions proteins and multimode FRET microscopy. J. Microsc. **214,** 190–200.

Wagner, G.J., and Hrazdina, G. (1984). Endoplasmic reticulum as a site of phenylpropanoid and flavonoid metabolism in *Hippeastrum*. Plant Physiol. **74,** 901–906.

Wanner, L.A., Li, G., Ware, D., Somssich, I.E., and Davis, K.R. (1995). The phenylalanine ammonia-lyase gene family in *Arabidopsis thaliana*. Plant Mol. Biol. **27,** 327–338.

Winkel, B.S.J. (2004). Metabolic channeling in plants. Annu. Rev. Plant Biol. **55,** 85–107.

Winkel-Shirley, B. (1999). Evidence for enzyme complexes in the phenylpropanoid and flavonoid pathways. Physiol. Plant. **107,** 142–149.

Wu, P., and Brand, L. (1994). Resonance energy transfer: Methods and applications. Anal. Biochem. **218,** 1–13.

Yegneswaran, S., Woods, G.M., Esmon, C.T., and Johnson, A.E. (1997). Protein S alters the active site location of activated protein C above the membrane surface. J. Biol. Chem. **272,** 25013–25021.